Kinetics of Increased Deformability of Deoxygenated Sickle Cells upon Oxygenation

Zhi Huang,* Leigh Hearne,* Cynthia E. Irby,* S. Bruce King,† Samir K. Ballas,‡ and Daniel B. Kim-Shapiro*
*Departments of Physics and †Chemistry, Wake Forest University, Winston-Salem, North Carolina 27109 USA;
and ‡Cardeza Foundation, Jefferson Medical College, Philadelphia, Pennsylvania 19107 USA

ABSTRACT We have examined the kinetics of changes in the deformability of deoxygenated sickle red blood cells when they are exposed to oxygen (O_2) or carbon monoxide. A flow-channel laser diffraction technique, similar to ektacytometry, was used to assess sickle cell deformability after mixing deoxygenated cells with buffer that was partially or fully saturated with either O_2 or carbon monoxide. We found that the deformability of deoxygenated sickle cells did not regain its optimal value for several seconds after mixing. Among density-fractionated cells, the deformability of the densest fraction was poor and didn't change as a function of O_2 pressure. The deformability of cells from the light and middle fraction increased when exposed to O_2 but only reached maximum deformability when equilibrated with supraphysiological O_2 concentrations. Cells from the middle and lightest fraction took several seconds to regain maximum deformability. These data imply that persistence of sickle cell hemoglobin polymers during circulation in vivo is likely, due to slow and incomplete polymer melting, contributing to the pathophysiology of sickle cell disease.

INTRODUCTION

Sickle cell anemia is caused by the replacement of glutamate by valine at the sixth position of the β-globin chain (Pauling et al., 1949; Ingram, 1956). This substitution causes sickle cell hemoglobin (HbS) to polymerize under hypoxic conditions, decreasing the deformability of the red cell (Embury et al., 1994). Erythrocyte deformability can influence the rate of entry into capillaries and affects the bulk viscosity of blood (Mohandas and Hebbel, 1994). Although deoxygenation has no effect on the deformability of normal cells, the deformability of sickle cells is greatly reduced in the absence of oxygen (O_2) or a similar ligand such as carbon monoxide (CO). The decrease in deformability upon deoxygenation of sickle cells is due to increased intracellular viscoelasticity resulting from hemoglobin polymerization (Mohandas and Hebbel, 1994). Thus, HbS polymerization contributes to microvascular occlusion characteristic of sickle cell disease (Eaton and Hofrichter, 1990; Noguchi and Schechter, 1985).

All observations involving the kinetics of HbS polymerization are well explained by the double nucleation mechanism (Ferrone et al., 1985a,b). The aggregation of HbS monomers (a hemoglobin tetramer) into a polymer is initially thermodynamically unfavorable for aggregates below a critical size but becomes more favorable as the aggregate grows past this size. The smallest aggregate formed by this homogeneous nucleation for which growth is thermodynamically favorable is called the critical nucleus. Heterogeneous nucleation involves the formation of additional polymer on the surface of an existing one. Once homogeneous nucleation forms a polymer, heterogeneous nucleation forms a network of polymers (a domain) from each critical nucleus. The formation of the critical nucleus is the rate-limiting step in polymer growth. Thus, the kinetics of polymerization are characterized by exponential growth that begins with a period in which so little polymer is present that there appears to be a delay (the delay time) between induction and the appearance of polymer.

The length of the delay time depends on the solubility of the HbS molecules, which can be varied by changing the temperature or ligand saturation. A simple, approximate empirical formula relates the delay time to the solubility (Hofrichter et al., 1976): $1/t_d = \lambda(c_o/c_s)^n$, where t_d is the delay time, c_0 is the total concentration of hemoglobin molecules, c_s is the solubility of the hemoglobin, and λ is a proportionality factor. The exponent, n, is found to be $\sim$30–40 under physiological conditions. Thus, the delay time is extremely sensitive to the supersaturation ratio, c_0/c_s. Since ligand saturation has a great effect on solubility, the delay time before polymerization and the time spent during circulation under hypoxic conditions play a large role in determining whether or not polymerization will occur. If the delay time is longer than the time during which some sickle cells are in hypoxic circulation, $\sim$10 s on the average (Altman and Ditmer, 1971; Mozzarelli et al., 1987), these cells may escape polymerization.

If polymer melting (depolymerization) does not occur upon reoxygenation at the lungs, the cells would not benefit by a delay time for polymerization. Red blood cell transit times have been reported to be on the order of 1 s in the lungs and 3 s in arterial circulation (Altman and Ditmer, 1971; Mozzarelli et al., 1987). More recently, a very large range, from 0.03 to 14.5 s, was measured for the transit time in the pulmonary capillaries (Hogg et al., 1994). These transit times and the kinetics of polymer melting are major determinants of whether or not polymers persist through cycles of circulation and whether or not there are polymers in the arterial circulation. The absence of a delay time observed during

Submitted November 4, 2002, and accepted for publication June 17, 2003.
Address reprint requests to Daniel B. Kim-Shapiro, Tel.: 336-758-4993; Fax: 336-758-6142; E-mail: shapiro@wfu.edu.

0006-3495/03/10/2374/10 $2.00

melting (Mozzarelli et al., 1987) has led to the prediction that melting upon reoxygenation at the lungs may be fast (Ferrone, 1994). Other early studies have indicated that melting is likely to be slow enough that polymers persist during circulation (Hofrichter et al., 1974; Moffat and Gibson, 1974; Messer et al., 1976). More recently, Briehl and co-workers have used differential interference contrast microscopy on an in vitro system to observe the growth and melting of HbS polymers (Samuel et al., 1990; Briehl, 1995). Melting was observed to take seconds to tens of seconds for completion and was described as a direct reversal of polymer growth. One preliminary report has also been made indicating that the rate of polymer melting does not depend linearly on the concentration of ligand, and these results imply persistence of the polymer through cycles in the circulation (Horiuchi et al., 2001). A careful study by Agarwal et al. (2002) has shown that polymer melting proceeds both at the ends in a ligand-independent manner and from the fiber sides in a manner that may depend nonlinearly on ligand concentration.

As the presence of polymers decreases the deformability of sickle red blood cells (Mohandas and Hebbel, 1994), one would expect that the kinetics of polymer melting will govern changes in the deformability of deoxygenated sickle cells when exposed to O_2 or a similar ligand. The deformability of oxygenated sickle red blood cells is generally lower than that for normal cells (due to membrane damage resulting from repeated sickling and unsickling, membrane bound hemoglobin, dehydration, and oxidative damage) and varies as a function of the fraction of dense cells in the blood and percentage of fetal hemoglobin, both between patients and over time for a given patient (Ballas and Smith, 1992; Ballas et al., 1989; Mohandas and Hebbel, 1994). In this study, we examine the rate that CO and O_2 can improve the deformability of sickle red cells. Our results indicate that this rate of improvement in deformability upon exposure to O_2 is probably insufficient for full recovery of deformability during reoxygenation at the lungs or even, perhaps, in the arterial circulation. Thus, sickle cell polymers probably do enter hypoxic tissues in some cells, and these cells cannot benefit from a prolonged delay time for polymerization.

MATERIALS AND METHODS

Sample preparation

Sickle venous blood was drawn from patients with sickle cell disease following federal regulations and guidelines. The blood was deoxygenated by alternate application of a vacuum and argon atmosphere. It was transferred into a sealed flask and air was pulled out by a vacuum pump for a few minutes until bubbles stopped forming. Argon was then flowed into the flask and a positive argon pressure was maintained for at least 1 min. The process was repeated until the blood was fully deoxygenated, which took a total of ~20 min. Absorption spectroscopy of the blood in the near infrared was used to confirm the completion of deoxygenation (Huang et al., 2001a). A Lambda 9 spectrometer (Perkin Elmer, Shelton, CT) with an integrating sphere was used to reduce artifacts due to light scattering. The amount of hemolysis was measured by comparing the absorption of the blood to that of the supernatant after sedimentation of the red cells. The blood contained 2% hemolysis before preparation, and the method of deoxygenation brought the level of hemolysis up to 12%. No further hemolysis was detected resulting from mixing or passage through the flow chamber. Hemolysis is not likely to affect the results of deformability measurements, as free hemoglobin is too small and the red cell ghosts have too low a relative index of refraction to affect the diffraction pattern. The deoxygenated blood was diluted ~50 times into deoxygenated buffer yielding a concentration of 0.1–0.14 mM in heme (or a final concentration of 0.05–0.07 mM in heme after mixing with ligand saturated buffer).

For all experiments, isotonic buffers were used so that concentrations reported in mM or μM refer to dissolved gas or heme. Fifty grams of dextran (Sigma-Aldrich, St. Louis, MO), 34 mL of distilled water, and 10 mL of OptiPrep (Nycomed Pharma, Asker, Norway) were added to 200 mL phosphate buffered saline (PBS) yielding an isotonic buffer with a viscosity of 19.6 cp and pH of 7.4. The pH was not affected by addition of blood. The viscosity of the buffer was measured using a calibrated Cannon-Ubbelohde Semi-MicroDilution Viscometer (Cannon Instrument, State College, PA) at room temperature. The buffer was deoxygenated by bubbling with nitrogen gas for at least 1 h. Fully saturated, oxygenated, and CO buffers were obtained by bubbling pure O_2 or CO gases through the buffers for at least 1 h. Partially saturated, 0.56 mM oxygenated buffer was obtained by performing a 2.5-fold dilution of 100% oxygenated buffer with deoxygenated buffer. The O_2 concentration in the oxygenated buffer was verified by an O_2 sensor (Ocean Optics, Dunedin, FL). The 50% saturated CO buffer (0.5 mM) was made by bubbling with a premixed tank that was balanced with 50% nitrogen gas mixture for at least 1 h. The effects on the kinetics of deformability changes of partially saturated buffers were studied to try to mimic physiological O_2 concentrations in the lungs. However, we were limited by the fact that we needed to have a significant excess of ligand (O_2 or CO) compared to hemes so the kinetics would remain pseudo-first order, and by the fact that when the cell concentration was too low, the quality of our diffraction pattern diminished.

To separate the cells by density, PBS and OptiPrep solution were added in different proportions to the sickle blood to adjust the density of the solution, so that after centrifugation, the cells with highest density, ~15% of the total sickle erythrocytes, formed a pellet at the bottom of the container, whereas the rest of the cells formed a layer at the top. The cells at the top were carefully removed and collected for further separation. The dense cells at the bottom were collected and washed using PBS buffer. The cells taken from the top were resuspended with a lower-density solution of PBS buffer and OptiPrep, and were centrifuged for a second time, so that after centrifugation, the cells with medium density, ~42% of the total, went to the bottom of the container, whereas a similar amount of the cells with lowest density went to the top. The light cells from the top were removed and washed with PBS buffer. The medium density cells were collected from the bottom and washed with PBS buffer. The light, medium-density, and dense cells were resuspended separately in small volumes of buffer that were used in the flow-channel diffraction experiment. The three portions of cells were then deoxygenated separately and diluted with deoxygenated, dextran-containing buffer (described above) to reach a heme concentration of 100 μM (or final concentration of 50 μM after mixing with oxygenated buffer). The density-fractionated cells were mixed with partially O_2-saturated buffer to give a final O_2 concentration of 0.28 mM, and the kinetics of these cells to regain their deformability after mixing was measured. The density-fractionated cells were also equilibrated with fully O_2-saturated buffer to give a final O_2 concentration of 1.4 mM. The deformability of the density-fractionated cells mixed with partially O_2-saturated buffer 6.5 s after mixing was compared with that of corresponding density fraction of cells equilibrated with fully saturated buffer. The p-value was calculated for each comparison pair using the paired t-test function with two-tailed distribution in Microsoft Excel to show the significance of their difference.

Experimental setup

The experimental setup is shown in Fig. 1. A syringe pump (PHD 2000, Harvard Apparatus, Holliston, MA) pushed two 10 mL syringes containing the diluted deoxygenated sickle blood in one and oxygenated or CO-saturated buffer in the other to achieve a final flow rate of 20 mL/min through the flow channel. The samples were mixed 1:1 using a homemade mixer followed by a 4.5 cm section of an in-line mixer whose outer diameter was 3/16 inch with 27 removable elements (Koflo, Cary, IL). Measurements conducted using the homemade mixer alone (that is without the Koflo in-line mixers) showed that very little mixing was achieved by the homemade mixer. The function of the homemade mixer was simply to combine the two solutions that needed to be mixed. To ensure complete mixing through the in-line mixer, a longer section with more removable elements was used to compare the resultant diffraction patterns to that of the shorter mixer. The longer mixer produced the same ellipticity in the diffraction pattern as that of the shorter mixer with a piece of tubing used to make up the volume difference. The effective dead time of the mixing was measured to be 0.6 s using the method described by Gibson (1969). The rate for reaction of sodium ascorbate (Fluka Chemical, Milwaukee, WI) and 2,6-dichlorophenolindophenol sodium salt dihydrate (Fluka Chemical) was measured using an Olis RSM spectrometer (Olis, Bogart, GA) in the same buffer as that used for the diffraction experiment. The reaction rate was used to determine the dead time of mixing in flow-channel setup by measuring the change in absorption probed by a Helium-Neon Laser (Metrologic Instruments, Bellmawr, NJ). The time it took for the mixture to move from the point of mixing to the observation point was varied by changing the length of the tubing between the in-line mixer and the flow channel. Longer tubing gave more time for the deoxygenated erythrocytes to regain their deformability of the oxygenated erythrocytes.

The flow-channel device used to conduct deformability measurements was used as described previously (Huang et al., 2001b). This method is based on the same principles as ektacytometry developed by Mohandas and others (Clark et al., 1983). All measurements were performed at room temperature (20°C). The mixed solution passed through a flow channel that was made by two pieces of Plexiglas plate held together with a thin sheet of plastic sandwiched in the middle. A rectangular piece of plastic film was slit off and the space left was used as the flow channel. The flow channel through which the erythrocytes traveled was 55 mM long, 3 mM wide, and 0.1 mM thick. The shear stress on the erythrocytes is proportional to the flow rate. An argon-ion laser (ILT Model 5500A, Ion Laser Technology, Salt Lake City, UT) operated at 457 nm passed through the flow channel perpendicularly, and projected the diffraction pattern of the cells onto a circular screen that was made by a metal plate with a circular hole at its center. Deformable cells elongate in the direction of the flow and produce an elliptical diffraction pattern that correlates with the ellipticity of the stressed cells (Groner et al., 1980). The diffraction pattern from unfractionated sickle cells is due to contributions from two populations: deformable sickle cells that respond in a similar way as normal cells, and irreversibly sickled cells that orient perpendicularly to the direction of flow and produce a circular or oblong (sideways) diffraction pattern (Bessis and Mohandas, 1977).

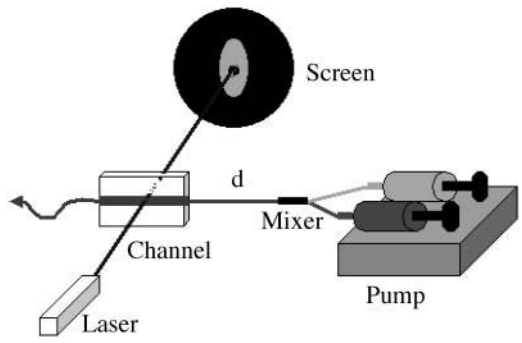

FIGURE 1 The experimental setup. The syringe pump pushed two syringes containing deoxygenated sickle erythrocytes in one and oxygenated or carbon monoxide (CO)-saturated buffer in the other to reach a final flow rate of 20 mL/min through the mixer into the flow channel. The mixer, composed of a homemade mixer followed by a 4.5 cm section of an in-line mixer, was used to achieve complete mixing of the two solutions. The time it took from the mixing to the observation point was varied by changing the length of the tubing (d) between the in-line mixer and the flow channel. Longer tubing gave longer times for the deoxygenated erythrocytes to regain their optimal deformability. The deformability was probed by measuring the diffraction pattern from a laser projected onto a screen.

Data collection and analysis

A DVC323 digital video camera (Eastman Kodak, Rochester, NY) recorded the diffraction patterns of the cells passing through the flow cell. The diffraction pattern was then analyzed using MATLAB software (The MathWorks, Natick, MA) to filter out noise and divide the major axis by the minor axis of the resultant elliptical shape. This axial ratio was defined as the deformability coefficient (DC). The diffraction patterns of the erythrocytes under the same flow rate were measured at different positions along the length of the flow channel to ensure that any entrance effect and differential shear stress along the length of the flow channel were insignificant and that the erythrocytes under the given shear stress were at equilibrium. For each experiment, the length of tubing with inner diameter of 1/8 inch (Fisher Scientific, Pittsburgh, PA) was varied between the mixer and the flow channel to vary the time between assessing the deformability and exposure to ligand (CO or O_2). No effect of the tube length on the deformability of either fully deoxygenated or fully ligated cells (that had not been dynamically mixed) was observed. After completion of each set of the experiments, the deformability at a certain tubing length was measured again to ensure reproducibility of the experiment. The result of the repeated measurement was always found to be consistent with that of the previous measurements.

To clearly show the kinetics of changes in the deformability after mixing in a background of large variability in the deformability from different blood samples, the data collected on fractionated cells were normalized by the maximum deformability for a given density fraction. This maximum deformability was obtained from measurements on the fractionated blood samples after equilibration with fully O_2-saturated buffer. The values for each density fraction were then multiplied by the average maximum deformability for all blood samples with that density. Thus, the calculated values are given by $\overline{DC}_{\mathrm{i}}^{\mathrm{norm}}(t) = ((DC_{\mathrm{i}}(t))/(DC_{\mathrm{i}}^{\mathrm{max}}))DC_{\mathrm{avg}}^{\mathrm{max}}$, where $DC_{\mathrm{i}}^{\mathrm{norm}}(t)$ is the normalized value of the deformability for a single measurement of a fractionated blood sample at a particular time after mixing, the subscript i refers to a particular blood sample, $DC_{\mathrm{i}}(t)$ is the unnormalized value of the DC for a single measurement of a fractionated blood sample, $DC_{\mathrm{i}}^{\mathrm{max}}$ is the maximum deformability for a single fractionated blood sample (that when equilibrated with 100% O_2-saturated buffer), and $DC_{\mathrm{avg}}^{\mathrm{max}}$ is the average maximum DC for all blood samples of a given fraction. The average value and standard deviation of $DC_{\mathrm{i}}^{\mathrm{norm}}(t)$ was then calculated for each density fraction, $\overline{DC}^{\mathrm{norm}}(t) = (1/N)\sum_{\mathrm{i}} DC_{\mathrm{i}}^{\mathrm{norm}}(t)$, where N is the number of blood samples and the index i is summed over all N blood samples.

RESULTS

Typical diffraction patterns formed from sickle cells in the flow chamber are shown in Fig. 2. The top pictures were taken on deoxygenated cells diluted into deoxygenated buffer that were passed through the flow channel without any dynamic mixing with another buffer. The middle and bottom

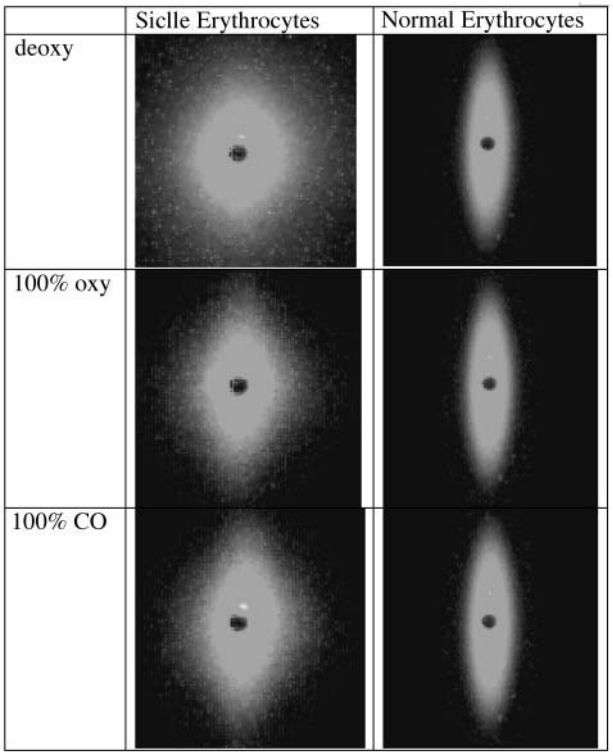

FIGURE 2 Diffraction patterns of sickle and normal erythrocytes: fully deoxygenated, fully oxygenated, and fully CO-saturated. The calculated deformability coefficients (DCs) for the sickle cells are 1.28 for 100% deoxygenated, 1.64 for fully oxygenated, and 1.73 for fully CO-saturated. The calculated DCs for the normal cells are 3.60 for 100% deoxygenated, 3.62 for 100% oxygenated, and 3.60 for fully CO-saturated.

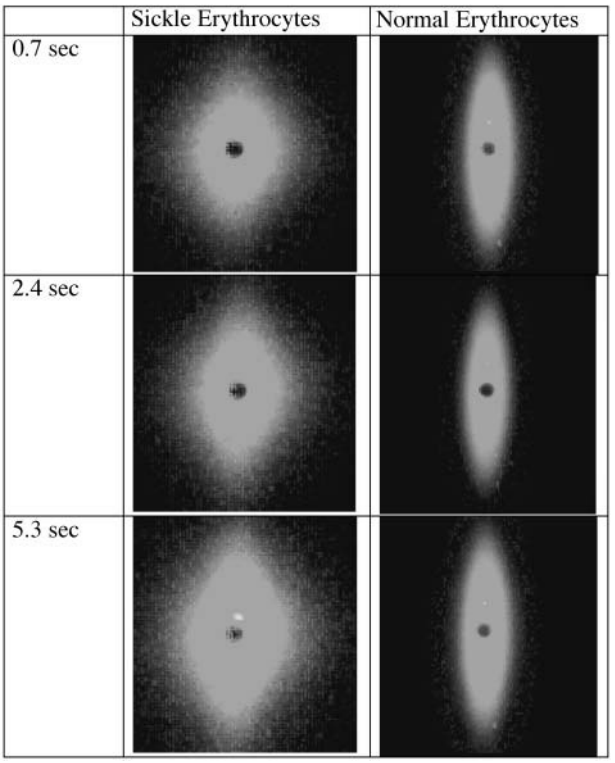

FIGURE 3 Diffraction patterns of sickle and normal erythrocytes of deoxygenated sickle erythrocytes mixed with oxygen (O_2, 0.70 mM) at various times after mixing. The calculated DCs for the sickle cells are 1.38 for 0.7 s, 1.58 for 2.4 s, and 1.64 for 5.3 s. The calculated DCs for the normal cells are 3.62 for 0.7 s, 3.58 for 2.4 s, and 3.59 for 5.3 s.

pictures correspond to cells that had been exposed to 1 atm O_2 or CO, diluted into buffers saturated with these gases, and then passed through the flow channel. The pattern for the deoxygenated sickle cells is nearly circular, indicating very poor deformability. Those patterns of the ligand-saturated sickle cells are more elliptical indicating improved deformability. Diffraction patterns for normal cells under identical conditions are shown on the right in Fig. 2. As expected, the deformability of normal cells is better than that of sickle cells, even at high ligand (O_2 or CO) pressures and does not depend on these ligand pressures. Fig. 3 depicts diffraction patterns typical of deoxygenated cells that were dynamically mixed with the O_2-saturated buffer at various times after mixing. The pattern of sickle cells has clearly not reached its maximal ellipticity 0.7 s after mixing. For comparison, the diffraction pattern for normal cells under the same conditions is also shown in Fig. 3 (*right*), and the expected lack of dependence on the time after mixing with O_2 is observed.

Changes in the deformability as a function of time after mixing deoxygenated sickle cells with O_2 or CO are summarized in Fig. 4. Here, the DC of deoxygenated sickle cells mixed with various buffers is plotted versus the time after dynamic mixing. Each trial was taken on a different day using cells from a different blood sample. Differences between samples are most likely due to differences in the deformability of the cells from individual patients as a result of different proportions of light and dense cells and different levels of fetal hemoglobin. In panels *A* and *B*, the average and standard deviations are shown for repeated measurements on a single blood sample (*trial 6* with *error bars* shown). The variability in repeated measurements on the same blood sample is much smaller than that between different blood samples. Panel *A* shows the results obtained when mixing with oxygenated buffer so that the concentration of O_2 after mixing was 0.28 mM. Panel *B* shows results obtained from mixing with partially CO-saturated buffer so that the CO concentration after mixing was 0.25 mM. Data collected when the deoxygenated cells were mixed with saturated O_2 (panel *C*) or CO (panel *D*) are also shown. In all the trials, the deformability had clearly not reached its maximum value at 0.7 s after mixing. The maximum DC appears to be reached faster at the higher, supraphysiological ligand pressures used in panels *C* and *D*. In the case of the lower (more physiologically relevant) ligand pressures, the cells often did not regain their maximum deformability until at least 5.3 s after mixing.

To reduce between sample variability due to the proportions of dense cells in different blood samples, we conducted studies on density-fractionated cells. Since the

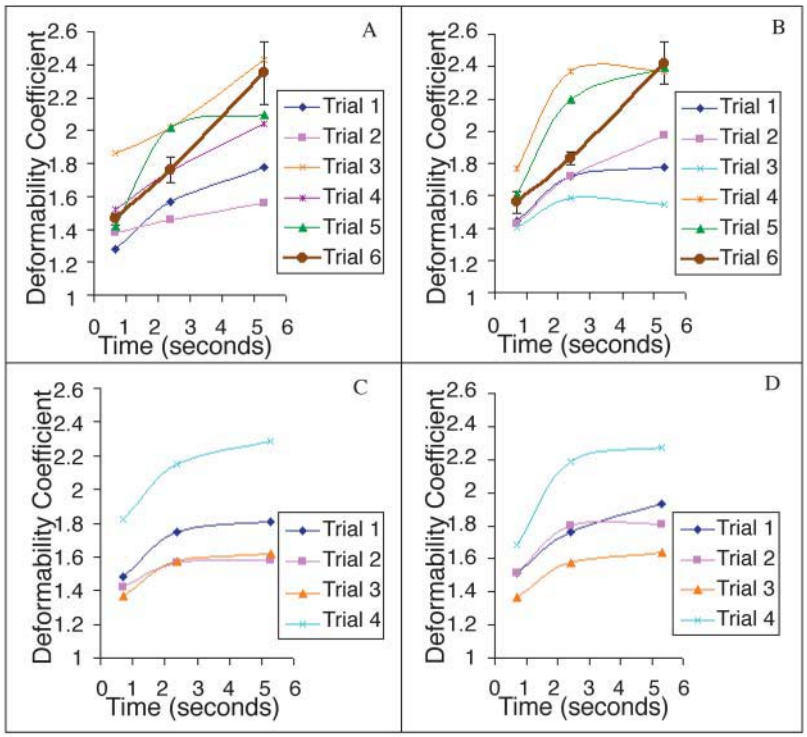

FIGURE 4 The DC of deoxygenated sickle erythrocytes mixed with oxygenated or CO-saturated buffer plotted against time after mixing. (*A*) Deoxygenated sickle erythrocytes were mixed with 0.56 mM oxygenated buffer to achieve a final O_2 concentration of 0.28 mM. The difference between the trials was due to different blood source, the freshness of the erythrocytes, and the storage time after deoxygenation. The error bars on trial 6 represent the standard deviation from two measurements on the same blood sample taken ~30 min apart. (*B*) Deoxygenated sickle erythrocytes were mixed with 50% CO-saturated buffer to reach a final concentration of dissolved CO of 25% (250 μM). The error bars on trial 6 represent the standard deviation from two measurements on the same blood sample taken ~30 min apart. (*C*) Deoxygenated sickle erythrocytes were mixed with 1.4 mM oxygenated (fully saturated) buffer to achieve a final O_2 concentration of 0.70 mM. (*D*) Deoxygenated sickle erythrocytes were mixed with 100% CO-saturated buffer to reach a final concentration of dissolved CO of 50% or 0.5 mM.

mixing with partially O_2-saturated buffer is most physiologically relevant, we conducted further studies on density-fractionated cells under these conditions. Fig. 5 shows the average change in deformability for density-fractionated cells when mixed with O_2 yielding a final O_2 concentration of 0.28 mM. The data were collected from five separate blood samples and the average normalized deformability coefficient, $\overline{DC}^{\text{norm}}(t)$, at each time after mixing was calculated as described in the Materials and Methods section. The deformability of the densest fraction of cells is seen not to change significantly upon mixing with the partially O_2-saturated buffer. The deformability of these dense cells is much lower than that for cells from the other fractions. The cells from the middle fraction did not regain their maximum deformability after mixing with the partially O_2-saturated buffer for at least 4 s. This deformability is still lower than that when this fraction of cells is equilibrated with fully O_2-saturated buffer as demonstrated in Fig. 6. When the cells from the least dense fraction were mixed with the partially O_2-saturated buffer, they did not regain their maximum deformability until at least 5 s after mixing with the partially O_2-saturated buffer (Fig. 5). Again, this maximum obtained with dynamic mixing with partially O_2-saturated buffer was significantly less than that when the light cells were equilibrated with 100% O_2 (Fig. 6).

Fig. 6 shows the comparison between the average deformability for density-fractionated cells 6.5 s after mixing with partially O_2-saturated buffer and the average deformability of the fractionated cells after equilibration with O_2-saturated buffer (1.4 mM). All data used here are the original data that have not been normalized. The dense fraction of cells has poorest deformability 6.5 s after mixing with partially O_2-saturated buffer and is not significantly changed when mixed with fully O_2-saturated buffer. The cells from

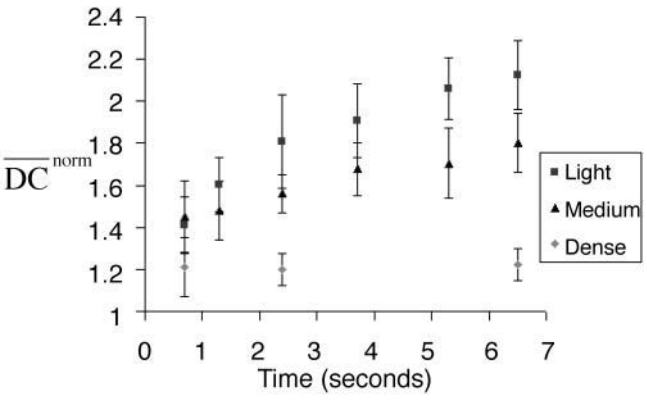

FIGURE 5 Normalized average DC of deoxygenated density-fractionated sickle erythrocytes mixed with partially O_2-saturated buffer plotted against time after mixing. Measurements were taken on five different blood samples and the normalized average deformability, $\overline{DC}^{\text{norm}}(t)$, was calculated as described in the Materials and Methods section. The deformability at each time after mixing was divided by the maximum deformability for that particular blood sample fraction obtained by equilibration with 100% O_2. This ratio is then multiplied by the average maximum deformability of all the blood samples for the particular fraction (light, medium, or dense). The average of these normalized deformabilities from five different blood samples are plotted with ±SD. Light, medium, and dense indicate the increase in density of the three density fractions of sickle erythrocytes. Each fraction of erythrocytes was deoxygenated and then mixed with 0.56 mM oxygenated buffer to achieve a final O_2 concentration of 0.28 mM.

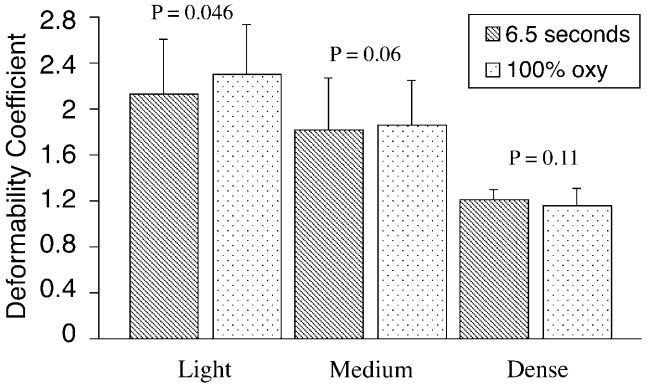

FIGURE 6 Average DC of deoxygenated density-fractionated sickle erythrocytes 6.5 s after mixing with partially O_2-saturated buffer compared with that of fully oxygenated erythrocytes for the same density fractions. The average and standard deviations were calculated from the original un-normalized data for five different blood samples. *p*-values were derived from a paired *t*-test.

the light and middle fractions 6.5 s after mixing with partially O_2-saturated buffer have significantly lower deformability than that when the cells were equilibrated with fully O_2-saturated buffer.

The results of a study of the effect of temperature on the kinetics of changes in deformability are shown in Fig. 7. For each blood sample, measurements were conducted at each temperature, 20°C and 37°C. Paired measurements were conducted on three different whole blood samples and the un-normalized average DC and standard deviations were

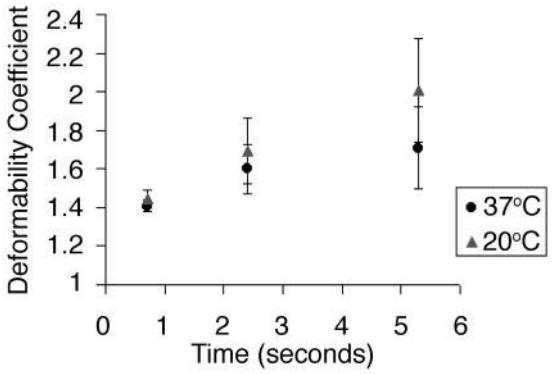

FIGURE 7 Average temperature effect on the DC of deoxygenated sickle erythrocytes mixed with partially O_2-saturated buffer plotted against time after mixing. The un-normalized average DC and standard deviations were calculated from three paired measurements, at 20°C and 37°C, and each measurement was conducted using a different blood sample. For the DC measurements at 37°C, the blood samples were incubated at 37°C for 30 min before use. The deformability of the samples after equilibration with 100% O_2-saturated buffer was the same at both temperatures; for example, on one blood sample, we measured DC = 2.16 at 37°C and 2.22 at 20°C. The average DC for samples equilibrated with 100% O_2 at 37°C DC was 2.09 ± 0.14. Further measurements at 37°C at 6.5 s after mixing gave a value of 1.74 ± 0.05, confirming that the deformability of the cells was still changing at 5.3 s where the DC was 1.71 ± 0.21 after mixing at this temperature.

calculated. The initial measured deformabilities at 0.7 s after mixing with partially oxygenated buffer were similar, but subsequent changes at 37°C were much slower than that at 20°C. The deformability of the samples after equilibration with 100% O_2-saturated buffer were the same at both temperatures, and further measurements at 37°C at 6.5 s after mixing confirmed that the deformability of the cells was still changing at 5.3 s after mixing at this temperature (data not shown).

DISCUSSION

We have examined the rate that deoxygenated sickle cells increase their deformability upon exposure to CO or O_2. We found that unfractionated sickle cells do not regain their maximal deformability at 0.7 s when mixed with fully O_2- or CO-saturated buffer, and when partially ligated buffers are used, the cells do not regain their normal deformability for several seconds after mixing. Further studies showed that cells with relatively light and medium density did not regain their maximum deformability for at least 4–6 s after mixing with partially oxygenated buffer.

Fig. 4 shows that, although reproducibility is very good when repeating measurements on a single blood sample, there is large variability in the deformability between trials made on different blood samples. This variability in the measured DC between different blood samples is consistent with that found previously for oxygenated samples (Ballas and Smith, 1992, Ballas et al., 1989). Ballas and Smith (1992) found that during crisis the DC can change dramatically where most of the ~100 patients studied had measured DCs between 1.3 and 3.8. (The deformability in the work was calculated using a deformability index (DI) equal to the ratio of the difference of the major and minor axes to their sum. We converted the DI values to our DC using the equation $DC = (DI + 1)/(1 - DI)$.)

In our studies, some of the blood that was drawn was from patients who probably were in crisis. Ballas and Smith found that the proportion of dense cells varied in concordance with changes in DC. This indicates that the major factor in the variability of the deformability between patients is due to the percentage of dense cells. Other factors that could contribute to variability in DC include the percentage of fetal hemoglobin as indicated by improvements in DC upon treatment with hydroxyurea (Ballas et al., 1989). Our data show that although we observe the expected variability in the equilibrium deformability of sickle red cells, the kinetics of the changes in the deformability as a function of time after exposure to O_2 or CO show consistent behavior, especially for fractionated cells.

The effects on the kinetics of deformability changes of partially saturated buffers were studied to try to mimic physiological O_2 concentrations in the lungs. The O_2 pressure in the lungs is actually such that its concentration in water would be <0.2 mM. However, under our most

physiologically relevant conditions, using partially O_2-saturated buffer (0.28 mM), the unfractionated sickle cells did not regain their optimal deformability until 2.4 s after mixing. Slower changes were observed for fractionated cells. Our observed slow changes in deformability measured at 0.28 mM O_2 are likely to be the same or (more likely) even slower below 0.2 mM.

Studies on fractionated cells revealed that cells from the densest fraction have very poor deformability that does not increase when mixed with partially oxygenated buffer or even when equilibrated with fully O_2-saturated buffer. Thus, consistent with previous findings (Bessis and Mohandas, 1977; Clark et al., 1980; Green et al., 1988; Noguchi et al., 1983), these dense cells are likely to contribute to poor rheology of sickle cell blood at all O_2 saturations. The cells from the medium fraction did increase their deformability when exposed to partially O_2-saturated buffer within 4–6 s after mixing. However, the maximum deformability achievable when these cells from the medium fraction were mixed with partially O_2-saturated buffer was less than that when the cells were equilibrated with 100% O_2-saturated buffer. Similarly, the cells from the light fraction did not regain their maximum deformability after mixing with partially oxygenated buffer for at least 5.3 s, and this maximum was significantly below that when the cells were equilibrated with 100% O_2-saturated buffer (Fig. 6). Thus, our data suggest that a fraction of sickle cells with less than their optimal deformability will persist during circulation, likely even into hypoxic tissue.

In general, several factors contribute to the deformability of sickle erythrocytes, including sickle polymer content, intrinsic rigidity of the membrane, amount of membrane-associated hemoglobin, and hydration of the cell (Evans and Mohandas, 1987; Hebbel et al., 1990; Clark et al., 1983, Sorette et al., 1987). The poor deformability of the dense cells is most likely due to intrinsic rigidity of these irreversibly sickled cells because their deformability was independent of exposure to O_2, which melts polymers. Of the various factors affecting deformability, the most likely rate-limiting factor governing our observed changes in sickle cell deformability is the rate of decrease in polymer content, e.g., the rate of sickle hemoglobin polymer melting. The other factors are not likely to change on the timescale of these measurements if they change at all upon exposure to ligand. The loss of ellipticity in the diffraction pattern of the deoxygenated cells may actually be due to sickled cells that orient perpendicular to the flow in a manner similar to irreversibly sickled cells or do not have any preferred orientation (Sorette et al., 1987). Alternatively, the cells may still orient parallel to the flow but not extend as much in the stress field. Either way, the loss of ellipticity in the diffraction pattern is correlated with poor deformability resulting from HbS polymerization. The rate of sickle hemoglobin polymer melting could be limited, in principle, by the ligand uptake rate of the cells or by an intrinsic polymer melting rate. However, the rate of ligand uptake is much too fast to be a rate-limiting step in our measurements of changes of deformability (Harrington et al., 1977; Olson, 1981; Hasinoff, 1981). Thus, the rate of changes in the deformability of sickle erythrocytes is most likely governed by the intrinsic rate of sickle hemoglobin melting. Our results from measurements on cells from the light and medium density fractions indicate that the polymers in these cells do not completely melt for at least 4–6 s when mixed with physiologically relevant O_2 pressures.

There has been some controversy over the degree of HbS polymerization that is required to affect the deformability of sickle erythrocytes (Mohandas and Hebbel, 1994). Studies using ektacytometry and cell aspiration to measure deformability as a function of O_2 tension found that a large amount of polymer is necessary to decrease the deformability of the cell (Nash et al., 1986; Itoh et al., 1992; Sorette et al., 1987). Studies based on the cells ability to traverse filters indicated that only a small amount of polymer can reduce sickle cell deformability (Green et al., 1988). The filter assay was stated to be more sensitive than ektacytometry or cell aspiration techniques (Green et al., 1988). Our assay is similar to ektacytometry so it is probable that the persistence of polymers is longer than that indicated by the time for changes in deformability measured in our experiments.

Our results imply that, in vivo, polymers persist after oxygenation at the lungs. Although our studies were conducted mainly at room temperature (20°C) on sickle cells that are completely deoxygenated, the polymer content of these cells was probably not very different from that found under physiological conditions. The O_2 pressures in the microcirculation and some venous circulations are found to be ~20 torr or less (Altman and Ditmer, 1971). Based on the reduced O_2 affinity of sickle cell blood (Eaton and Hofrichter, 1994), this would correspond to hemoglobin O_2 saturations ranging from 10% to 15%. The oxygen saturation of mixed venous blood in patients with sickle cell disease ranges from 25% to 75% (Poillon et al., 1993, Klug et al., 1974). Using an empirical equation derived by Eaton and Hofrichter relating the solubility to the temperature and O_2 saturation (1990), we find that the solubility at 20°C and an oxygenation saturation of 0% gives a solubility of 0.194 g/mL, which would correspond to the solubility at 37°C for an oxygenation saturation of 29%. Thus, based on these calculations of the solubility at equilibrium, the O_2 pressure we worked with at 20°C would yield less polymer than that found in the microcirculation and be equivalent to those at the lower O_2 saturations found in mixed venous blood. For sickle cells with an average total intracellular hemoglobin concentration (0.34 g/mL), the fraction of polymerized hemoglobin in the cell at 37°C only decreases by a factor of 1.3 when the hemoglobin O_2 saturation is increased from 30% to 50% and would increase even less for denser cells (Noguchi et al., 1980). In principle, the rate of deoxygenation of the blood in our studies could also produce polymer

domains of different types and sizes from those found in vivo. Slow deoxygenation will produce fewer, slowly melting, large polymer domains (as opposed to more, rapidly melting, small domains) than fast deoxygenation (Louderback et al., 1999). However, the variation in the size of the domains for the current report are limited by the size of the red cell, whereas in our 1999 work, we were able to achieve domains with dimensions of the order of several millimeters (Louderback et al., 1999). Moreover, Mickols et al. (1988) found that the presence of preformed nucleation sites at ambient O_2 tensions greatly reduces any effect of the speed of deoxygenation on the amount of aligned polymer and, hence, the nature of the domains in sickle red cells. In addition, the domain size will depend on the concentration of HbS within the cell as well, and the variation of density of sickle red blood cells leads to a multitude of sickle cell morphologies found in vivo (Corbett et al., 1995). Thus, the difference in cell and domain structures in our experiments and those found in vivo are likely to be in a slight shift in proportions of the different types.

In addition to affecting the equilibrium amount of polymer, temperature affects the rate of melting. In previous studies in a model system (1.8 M phosphate), we have found that increasing the temperature from 20°C to 37°C slows down the rate of polymer melting (Louderback et al., 1999), consistent with the increased stabilization of the polymer phase at 37°C. In Fig. 7, we show that when the experiments were performed mixing deoxygenated cells and oxygenated buffer that had been equilibrated at 37°C, the rate of changes in the deformability is slower than for the same samples when equilibrated at 20°C. The decrease in the rate of polymer melting at 37°C could be due to either more polymer, and hence larger domains formed at this temperature, or slower polymer melting, consistent with our earlier work (Louderback et al., 1999). However, even though the solubility decreases from 0.19 g/mL to 0.165 g/mL when increasing the temperature from 20°C to 37°C (Eaton and Hofrichter, 1990), the polymer fraction for sickle cells of average mean cell hemoglobin concentration (0.34 g/mL) only increases by a factor of 1.1 (Noguchi et al., 1980). (The polymer fraction was calculated using the equations described by Noguchi et al. in their Eqs. 1 and 2. Briefly, the total hemoglobin is expressed as the sum of that in the polymer phase and in the solution phase. The fraction in each phase is equal to its concentration times its volume fraction divided by the total hemoglobin concentration. The concentration of hemoglobin in the polymer phase is 0.7 g/mL, and we used the concentrations in the solution phase calculated according to the equations of Eaton and Hofrichter (1990). Generally, a given change in solubility often does not correspond to as large a change in polymer fraction because the solubilities described are much smaller than the total hemoglobin in the cells.) Thus, the slower kinetics of polymer melting seen at 37°C are most likely mainly due to an intrinsically lower rate of melting at this temperature rather than an increase in polymer content or domain size. The slow kinetics shown in Fig. 7 for data taken at 37°C are likely to correspond to what happens at this physiological temperature even though there was slightly more polymer (since the experiments were performed with cells that started out fully deoxygenated) than usually found in vivo.

Another difference between the conditions used in our studies and those found in vivo stems from the effects of carbon dioxide (CO_2). Unlike in vivo, our samples were not exposed to any CO_2. The effects of CO_2 on HbS polymerization are complicated (Ueda and Bookchin, 1984). The ability of CO_2 to decrease the pH and bind preferentially to deoxygenated Hb enhances polymerization, whereas the binding itself also partially inhibits polymerization. The magnitude of these opposing effects depends on the concentration of CO_2 and pH (Ueda and Bookchin, 1984). It is known that the intracellular pH of sickle cells is lower than that of normal cells: 7.1–7.2 for sickle cells compared to 7.2–7.3 for normal cells (Kaperonis et al., 1979; Ueda et al., 1979). Thus, the pH used in our studies (7.4) was slightly higher than that relevant to in vivo conditions, which would decrease the extent of polymerization in our studies compared to in vivo. We believe that, in vivo, CO_2 would generally decrease the amount of polymerization compared to that found in our studies, whereas the lower pH found in vivo would have the opposite effect, and that the overall effects of these would not change our general conclusion that polymers persist after oxygenation at the lungs. Further work may be required to confirm this belief.

One of the effects of persistence of the polymers in vivo would be an increase in the bulk viscosity of sickle cell blood. The red cells' deformability makes blood a highly non-Newtonian fluid, so that the viscosity is highly dependent on the shear rate (Mohandas and Hebbel, 1994). Whereas deoxygenation has no effect on normal blood, it causes an order-of-magnitude increase in viscosity of sickle blood (Mohandas and Hebbel, 1994). If bulk viscosity increases, flow rate and, hence, shear rate can decrease, leading to an additional increase in viscosity (due to the non-Newtonian behavior of blood). Decreased flow rate can lead to increased hypoxia and sickling, which then lead to occlusion, which furthers hypoxia. Thus, the deformability of red cells is one of the defining factors in *two coupled vicious cycles* that contribute to the pathophysiology of sickle cell disease. The effects of slow polymer melting upon oxygenation at the lungs can be compounded through these coupled vicious cycles and the prevention of a delay time in some cells that enter relative hypoxia.

The most important implication of persistence of the polymers after oxygenation at the lungs may be due to their contribution to occlusion events. Generally, there could be some sickle cells that always contain polymers even in equilibrium at all physiological O_2 pressures, some sickle cells that would never sickle due to their low HbS content, and some sickle cells that escape sickling due to their delay

times. Use of ^{13}C NMR techniques to examine intracellular polymer content has shown that some cells contain polymers at >90% HbO_2 saturation (Noguchi et al., 1980, 1983), a higher oxygen saturation than that found in the arterial circulation of some patients with sickle anemia (Jensen et al., 1957). This result is consistent with our studies indicating incomplete polymer melting upon exposure to 0.28 mM O_2 in cells from light and medium fraction. As pointed out by Mozzarelli et al. (1987), slow depolymerization could reduce the number of sickle cells that escape polymerization due to a delay time in sickling. Our study indicates that polymer melting is not likely to be complete during the second or so spent at the lungs and is probably not complete during arterial circulation. This would increase the proportion of sickled cells and contribute to occlusion events. Possible future therapeutic interventions could include agents that melt polymers quickly.

The authors thank Constance T. Noguchi and Alan N. Schechter for helpful discussion, and Frank Ferrone for helpful discussions about double nucleation theory.

This work was supported by National Institutes of Health grant HL58091 (D.B.K.-S.) and the Wake Forest University Catalyst Award (D.B.K.-S. and S.B.K.). Additional support was obtained from National Institutes of Health grant HL62198 (S.B.K.) and the Comprehensive Sickle Cell Program of the Commonwealth of Pennsylvania (S.K.B.).

REFERENCES

Agarwal, G., J. C. Wang, S. Kwong, S. M. Cohen, F. A. Ferrone, R. Josephs, and R. W. Briehl. 2002. Sickle hemoglobin fibers: mechanisms of depolymerization. *J. Mol. Biol.* 322:395–412.

Altman, P. A., and D. S. Ditmer. 1971. Respiration and circulation. *Federation of American Society of Experimental Biologists, Bethesda, MD*. 417–422:498.

Ballas, S. K., G. I. Dover, and S. Charache. 1989. The effect of hydroxyurea on the rheological properties of sickle erythrocytes in vivo. *Am. J. Hematol.* 32:104–111.

Ballas, S. K., and E. D. Smith. 1992. Red cell changes during the evolution of the sickle cell painful crisis. *Blood.* 79:2154–2163.

Bessis, M., and N. Mohandas. 1977. Laser diffraction patterns of sickle cells in fluid shear fields. *Blood Cells.* 3:229–239.

Briehl, R. W. 1995. Nucleation, fiber growth and melting, and domain formation and structure in sickle cell hemoglobin gels. *J. Mol. Biol.* 245:710–723.

Clark, M. R., N. Mohandas, and S. B. Shohet. 1980. Deformability of oxygenated irreversibly sickled cells. *J. Clin. Invest.* 65:189–196.

Clark, M. R., N. Mohandas, S. B. Shohet, R. M. Hoesch, and M. E. Rossi. 1983. Osmotic gradient ektacytometry-comprehensive characterization of red-cell volume and surface maintenance. *Blood.* 61:899–910.

Corbett, J. D., W. E. Mickols, and M. F. Maestre. 1995. Effect of hemoglobin concentration on nucleation and polymer formation in sickle red blood cells. *J. Biol. Chem.* 270:2708–2715.

Eaton, W. A., and J. Hofrichter. 1990. Sickle cell hemoglobin polymerization. *Adv. Protein Chem.* 40:63–279.

Eaton, W. A., and J. Hofrichter. 1994. Sickle hemoglobin polymerization. *In* Sickle Cell Disease. S. H. Embury, R. P. Hebbel, N. Mohandas, and M. H. Steinberg, editors. Raven Press, New York. 53–87.

Embury, S. H., R. P. Hebbel, M. H. Steinberg, and N. Mohandas. 1994. Pathogenesis of vasocclusion. *In* Sickle Cell Disease. S. H. Embury, R. P. Hebbel, N. Mohandas, and M. H. Steinberg, editors. Raven Press, New York. 311–326.

Evans, E. A., and N. Mohandas. 1987. Membrane-associated sickle hemoglobin: a major determinant of sickle erythrocyte rigidity. *Blood.* 70:1443–1449.

Ferrone, F. A. 1994. Oxygen transits and transports. *In* Sickle Cell Disease. S. H. Embury, R. P. Hebbel, N. Mohandas, and M. H. Steinberg, editors. Raven Press, New York. 89–98.

Ferrone, F. A., J. Hofrichter, and W. A. Eaton. 1985a. Kinetics of sickle hemoglobin polymerization. I. Studies using temperature jump and laser photolysis techniques. *J. Mol. Biol.* 183:591–610.

Ferrone, F. A., J. Hofrichter, and W. A. Eaton. 1985b. Kinetics of sickle hemoglobin polymerization. II. A double nucleation mechanism. *J. Mol. Biol.* 183:611–631.

Gibson, Q. H. 1969. Rapid mixing: stopped flow. *Methods Enzymol.* 16:187–228.

Green, M. A., C. T. Noguchi, A. J. Keiden, S. S. Marwah, and J. Stuart. 1988. Polymerization of sickle cell hemoglobin at arterial oxygen saturation impairs deformability. *J. Clin. Invest.* 81:1669–1674.

Groner, W., N. Mohandas, and M. Bessis. 1980. New optical technique for measuring erythrocyte deformability with the ektacytometer. *Clin. Chem.* 26:1435–1442.

Harrington, J. P., D. Elbaum, R. M. Bookchin, J. B. Wittenberg, and R. L. Nagel. 1977. Ligand kinetics of hemoglobin S containing erythrocytes. *Proc. Natl. Acad. Sci. USA.* 74:203–206.

Hasinoff, B. B. 1981. Kinetics of carbon monoxide and oxygen binding to hemoglobin human red blood cell suspensions studied by laser photolysis. *Biophys. Chem.* 13:173–179.

Hebbel, R. P., A. Leung, and N. Mohandas. 1990. Oxidation-induced changes in microrheologic properties of the red blood cell membrane. *Blood.* 76:1015–1020.

Hofrichter, J., P. D. Ross, and W. A. Eaton. 1974. Kinetics and mechanism of deoxyhemoglobin S gelation: a new approach to understanding sickle cell disease. *Proc. Natl. Acad. Sci. USA.* 71:4864–4868.

Hofrichter, J., P. D. Ross, and W. A. Eaton. 1976. Supersaturation in sickle cell hemoglobin solutions. *Proc. Natl. Acad. Sci. USA.* 73:3035–3039.

Hogg, J. C., H. O. Coxson, M.-L. Brumwell, N. Beyers, C. M. Doerschur, W. MacNee, and B. R. Wiggs. 1994. Erythrocyte and polymorphonuclear transit time and concentration in human pulmonary capillaries. *J. Appl. Physiol.* 77:1795–1800.

Horiuchi, K., J. Hergert, and K. Ohene-Frempong. 2001. Unsickling of individual sickled cells at arterial oxygen tension. *The National Sickle Cell Disease Program, 25th Annual Meeting*. National Institutes of Health/National Heart, Lung, and Blood Institute. A168.

Huang, Z., J. G. Louderback, F. Azizi, M. Goyal, S. Bruce King, and D. B. Kim-Shapiro. 2001a. Nitric oxide binding to hemoglobin under physiological conditions. *Biophy. Biochem. Acta.* 1568:252–260.

Huang, Z., J. G. Louderback, S. B. King, S. K. Ballas, and D. B. Kim-Shapiro. 2001b. Hydroxyurea reduces the deformability of sickle red blood cells in vitro. *Am. J. Hematol.* 67:151–156.

Ingram, V. M. 1956. A specific chemical difference between the globins of normal human and sickle cell anemia hemoglobin. *Nature*. 178:792–794.

Itoh, T., S. Chien, and S. Usami. 1992. Deformability measurements on individual sickle cells using a new system with pO_2 control. *Blood.* 79:2141–2147.

Jensen, W. N., D. C. Rucknagel, and W. J. Taylor. 1957. Arterial oxygen unsaturation and possible mechanism of its production in sickle cell anemia. *J. Clin. Invest.* 37:905–906.

Kaperonis, A. A., J. F. Bertles, and S. Chien. 1979. Variability of intracellular pH within individual populations of SS and AA erythrocytes. *Br. J. Haematol.* 43:391–400.

Klug, P. P., L. S. Lessin, and B. S. Radice. 1974. Rheological aspects of sickle cell disease. *Arch. Intern. Med.* 133:577–590.

Louderback, J. G., S. K. Aroutiounian, W. C. Kerr, S. K. Ballas, and D. B. Kim-Shapiro. 1999. Temperature and domain size dependence of sickle

cell hemoglobin polymer melting in high concentration phosphate buffer. *Biophys. Chem.* 80:21–30.

Messer, M. J., J. A. Hahn, and T. B. Bradley. 1976. The kinetics of sickling and unsickling of red cells under physiological conditions: rheologic and ultrastructural correlations. *In* Proceedings of the Symposium on Molecular and Cellular Aspects of Sickle Cell Disease. J. I. Hercules, G. L. Cottam, M. R. Waterman, and A. N. Schechter, editors. Department of Health, Education, and Welfare Publ. No. (NIH) 76-1007, Bethesda, MD. 225–234.

Mickols, W. E., J. D. Corbett, M. F. Maestre, I. Tinoco, Jr., J. Kropp, and S. H. Embury. 1988. The effect of speed of deoxygenation on the percentage of aligned hemoglobin in sickle cells. Application of differential polarization microscopy. *J. Biol. Chem.* 263:4338–4346.

Moffat, K., and Q. H. Gibson. 1974. The rates of polymerization and depolymerization of sickle cell hemoglobin. *Biochem. Biophys. Res. Commun.* 61:237–242.

Mohandas, N., and R. P. Hebbel. 1994. Erythrocyte deformability, fragility and rheology. *In* Sickle Cell Disease. S. H. Embury, R. P. Hebbel, N. Mohandas, and M. H. Steinberg, editors. Raven Press, New York. 205–216.

Mozzarelli, A., J. Hofrichter, and W. A. Eaton. 1987. Delay time of hemoglobin S gelation prevents most cells from sickling in vivo. *Science.* 237:500–506.

Nash, G. B., C. S. Johnson, and H. J. Meiselman. 1986. Influence of oxygen tension on the viscoelastic behavior of red blood cells in sickle cell disease. *Blood.* 67:110–118.

Noguchi, C. T., and A. N. Schechter. 1985. Sickle hemoglobin polymerization in solution and in cells. *Annu. Rev. Biophys. Biophys. Chem.* 14:239–263.

Noguchi, C. T., D. A. Torchia, and A. N. Schechter. 1983. Intracellular polymerization of sickle hemoglobin. effects of cell heterogeneity. *J. Clin. Invest.* 72:846–852.

Noguchi, C. T., D. A. Torchia, and A. N. Schechter. 1980. Determination of deoxyhemoglobin S polymer in sickle erythrocytes upon deoxygenation. *Proc. Natl. Acad. Sci. USA.* 77:5487–5491.

Olson, J. S. 1981. Stopped-flow, rapid mixing measurements of ligand binding to hemoglobin and red cells. *Methods Enzymol.* 76:631–651.

Poillon, W. N., B. C. Kim, G. P. Rodgers, C. T. Noguchi, and A. N. Schechter. 1993. Sparing effect of hemoglobin F and hemoglobin A_2 on the polymerization of hemoglobin S at physiological ligand saturations. *Proc. Natl. Acad. Sci. USA.* 90:5039–5043.

Pauling, L., H. A. Itano, S. J. Singer, and I. C. Wells. 1949. Sickle cell anemia, a molecular disease. *Science.* 111:543–548.

Samuel, R. E., E. D. Salmon, and R. W. Briehl. 1990. Nucleation and growth of fibres and gel formation in sickle cell hemoglobin. *Nature.* 345:833–835.

Sorette, M. P., M. G. Lavenant, and M. R. Clark. 1987. Ektacytometric measurement of sickle cell deformability as a continuous function of oxygen tension. *Blood.* 69:316–323.

Ueda, Y., and R. M. Bookchin. 1984. Effects of carbon dioxide and pH variations in vitro on blood respiratory functions, red blood cell volume, transmembrane pH gradients, and sickling in sickle cell anemia. *J. Lab. Clin. Med.* 104:146–159.

Ueda, Y., R. L. Nagel, and R. M. Bookchin. 1979. An increased Bohr effect in sickle cell anemia. *Blood.* 53:472–480.